Supplemental Table 3. Antibody List and Panels

Marker	Fluor	Company	Catalogue #	Panel	Dilution Factor
CD8a	BV421	Biolegend	100753	1	1:200
CD44	Alexa Fluor 647	Biolegend	103018	1	1:600
Ghost	Red 780	Tonto Biosciences	13-0865-T100	1 &2	1:200
CD45	BV605	Biolegend	103155	2	1:200
CD4	BV510	Biolegend	100449	2	1:200
CD8	PerCP	Biolegend	100731	2	1:200
CD3	BV421	Biolegend	100335	2	1:50
CD69	FITC	Biolegend	104505	2	1:400
Tim3	PE-Cy7	Biolegend	119715	2	1:300
PD1	PE	Biolegend	135205	2	1:300
CD44	Alexa Fluor 700	Biolegend	103125	2	1:100

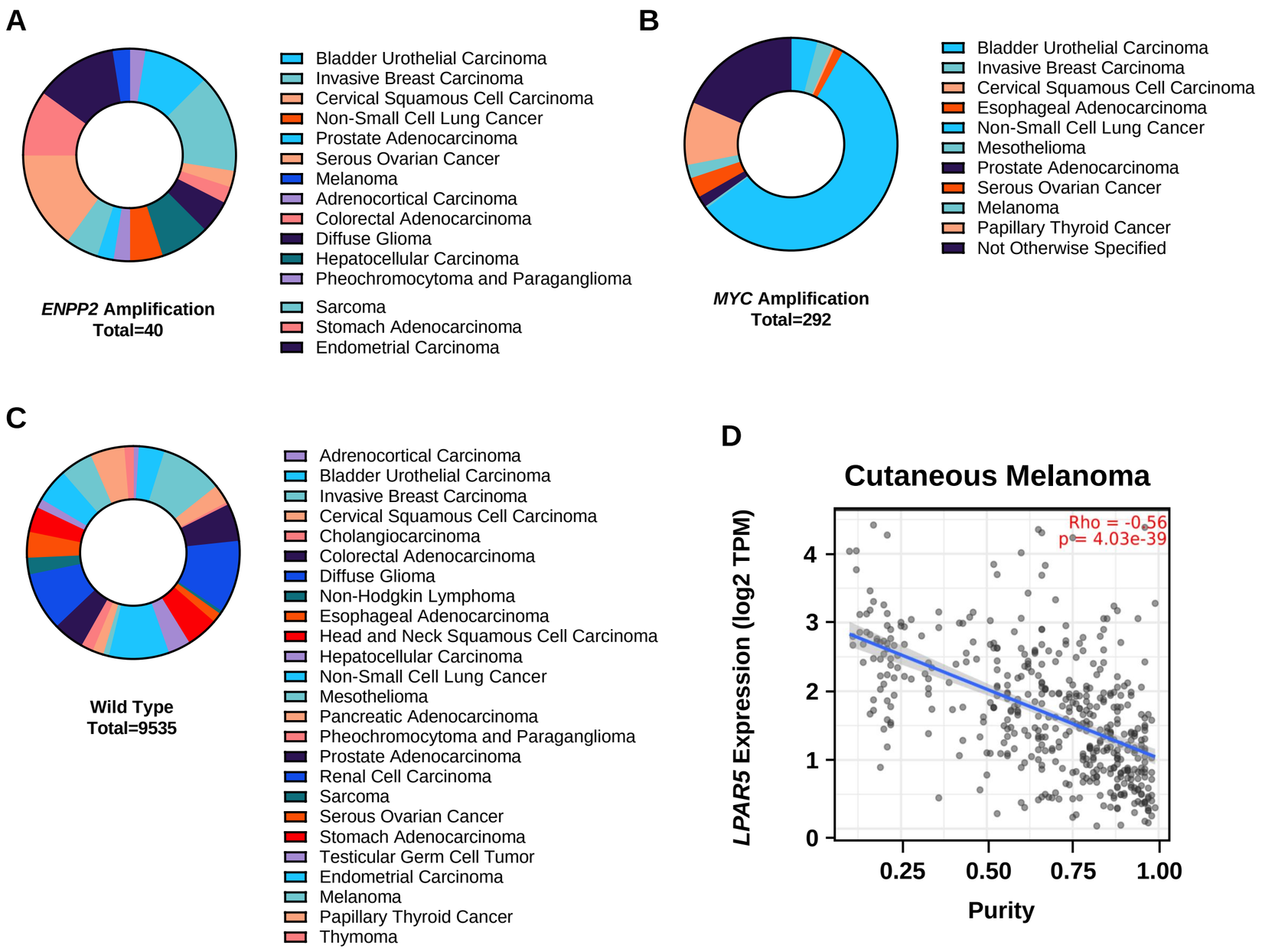

Supplemental Figure 1. Assessing cancer types from TCGA harboring *ENPP2* amplification and tumor purity with *LPAR5* expresison. (A,B,C) Graphic showing the distribution of cancer types from Figure 6 with *ENPP2* amplification where (A) represents tumors harboring an *ENPP2* amplification, (B) represents tumors harboring a *MYC* amplification, and (C) represents tumors that were wildtype for both *ENPP2* and *MYC*. Data demonstrate there are a spread of different cancer types with *ENPP2* amplification. (D) Correlation analysis of *LPAR5* expression and sample purity from cutaneous melanoma samples using TIMER2.0 (http://timer.cistrome.org/).

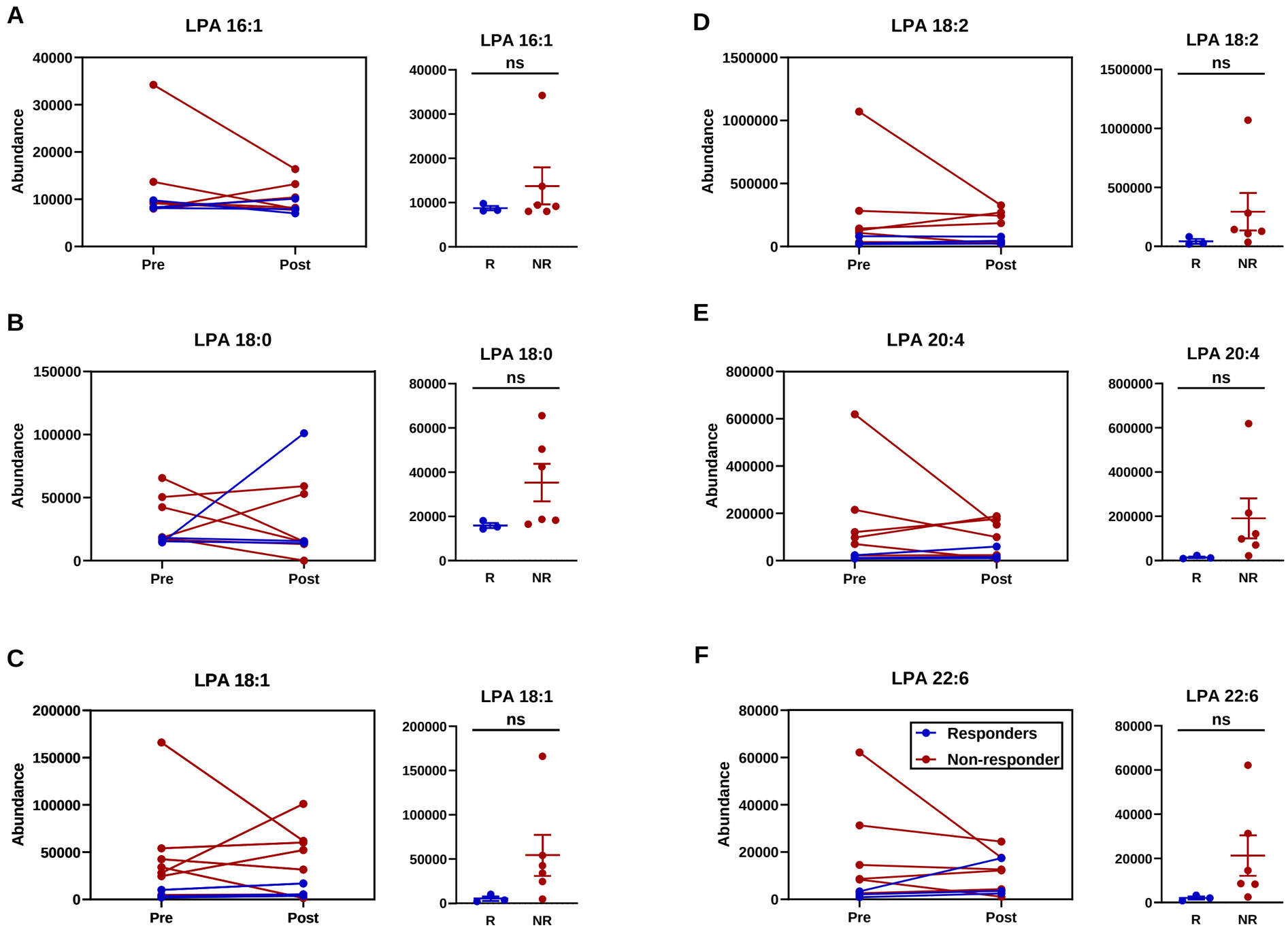

Supplemental Figure 2. Paired and unpaired analysis of plasma lysophosphatidic acid from stage IV melanoma patients from Figure 6. (A,B,C,D,E,F) Lipid abundances were determined for LPA molecular species in patients pre- and post-therapy including (A) 16:1, (B) 18:0, (C) 18:1, (D) 18:2, (E) 20:4, and (F) 22:6. R = responder and NR = non-responder. The unpaired and paired Student's t test analyses were performed where ns stands for not significant.

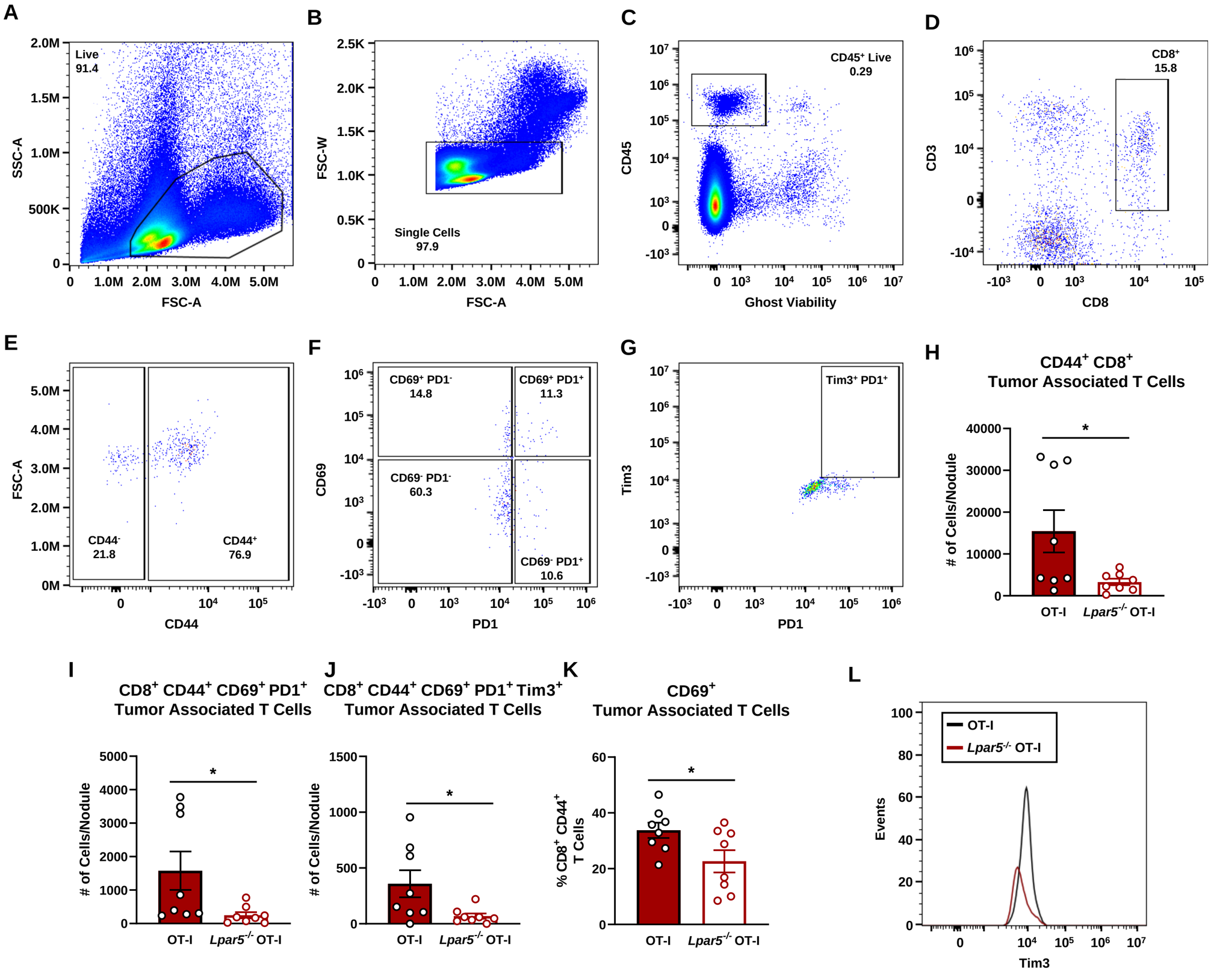

Supplemental Figure 3. Gating scheme and quantification of tumor associated T cells from Figure 5. (A,B,C,D,E) Tumor associated T cells were enumerated for after gating on (A) Live, (B) single cells, (C) $CD45^+$ Live (D) $CD3^+$ $CD8^+$ (E) $CD44^+$. (F,G) Cells were then further stratified based on exhaustion markers gating for either (F) $CD69^+$ $PD1^+$ or (G) $Tim3^+$ $PD1^+$. CD44, CD69, PD1, and Tim3 gates were determined using FMO gating. (H,I,J) The number of tumor associated CD8 T cells per nodule was quantitated for (H) total $CD8^+$ $CD44^+$, (I) $CD69^+$ $PD1^+$, and (J) $Tim3^+$ $PD1^+$. (K) Percent of $CD69^+$ tumor associated T cells graphed from the percent of $CD45^+$ Live then $CD8^+$ $CD44^+$. (L) Tim3 gMFI graphed from the percentage of cells from panel K. Statistics for this entire figure were performed using the unpaired Student's t test analysis was performed where * $p < 0.05$.

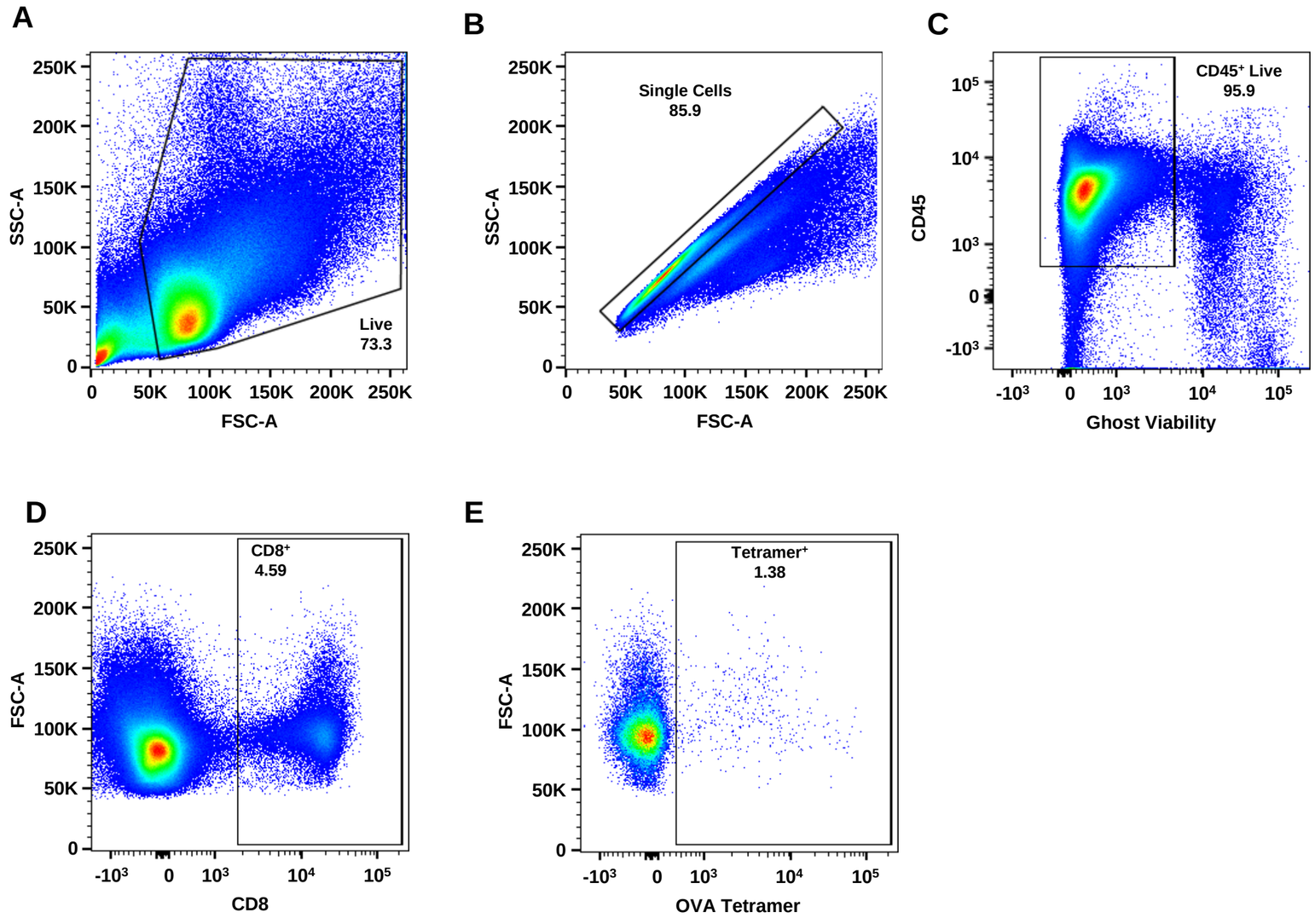

Supplemental Figure 4. Gating schematic for identifying tetramer$^+$ CD8 T cells after vaccination. Tetramer$^+$ CD8 T cells were enumerated in Figure 4 and first splenocytes were gated on (A) forward and side scatter (B) single cells (C) CD45$^+$ live (D) CD8$^+$ and then (E) Tetramer$^+$. Gating on Tetramer$^+$ CD8 T cells was determined based on fluorescence minus one (FMO) gating.

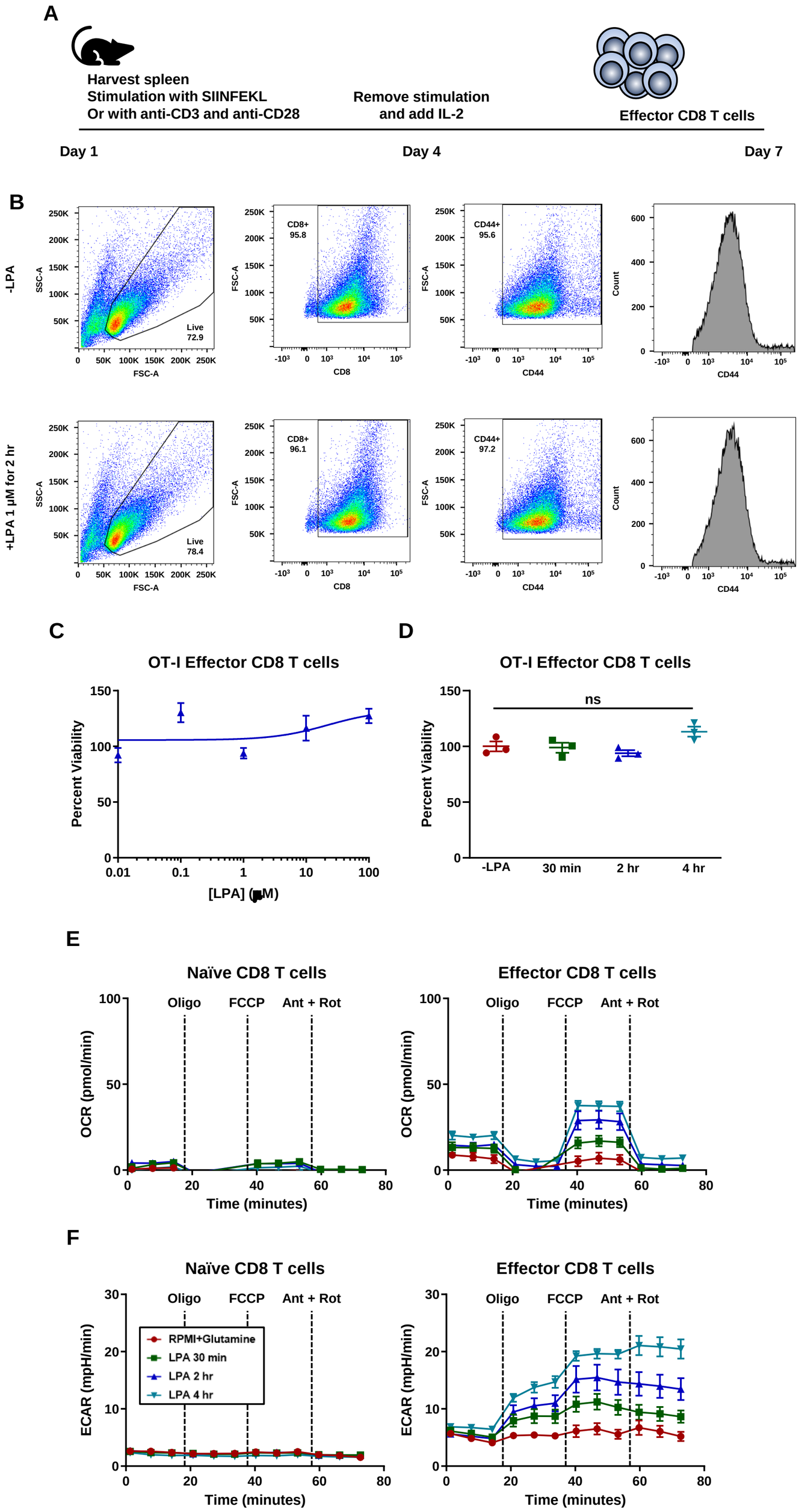

Supplemental Figure 5. Lysophosphatidic acid does not affect surface expression of CD8 and CD44, viability, or show obvious metabolic differences in CD8 T cells generated from anti-CD3 and anti-CD28 stimulation.(A) Generation of effector CD8 T cells ex vivo. Mice are harvested and CD8 T cells are activated with either SIINFEKL (N4) with other splenocytes serving as antigen presenting cells or plate bound anti-CD3 and anti-CD28. The N4 or anti-CD3 and anti-CD28 are removed on Day 4 and replaced with IL-2. In the presence of IL-2, the CD8 T cells differentiate and expand into effectors which are used for flow cytometric analysis of day 7 effector CD8 T cells that are homogenous at this time after *in vitro* culture. (B) T cells are gated as lymphocytes, $CD8^+$, $CD44^+$. Expression of CD8 and CD44 is unchanged with LPA treatment. (C,D) Viability of day 7 effector CD8 T cells treated with (D) varying concentrations of LPA or (D) 1 µM LPA for 30 minutes, 2 hours, or 4 hours. CD8 T cell viability is largely unchanged with the treatment of LPA. (E,F) Seahorse showing (E) oxygen consumption rate (OCR) and (F) extracellular acidification rate (ECAR) on C57BL/6 naïve CD8 T cells or day 7 effector CD8 T cells generated from anti-CD3 and anti-CD28 stimulation. Similar to OT-I CD8 T cells, the naïve CD8 T cells are metabolically quiescent, and the effector CD8 T cells also display increased OCR and ECAR in response to LPA treatment.

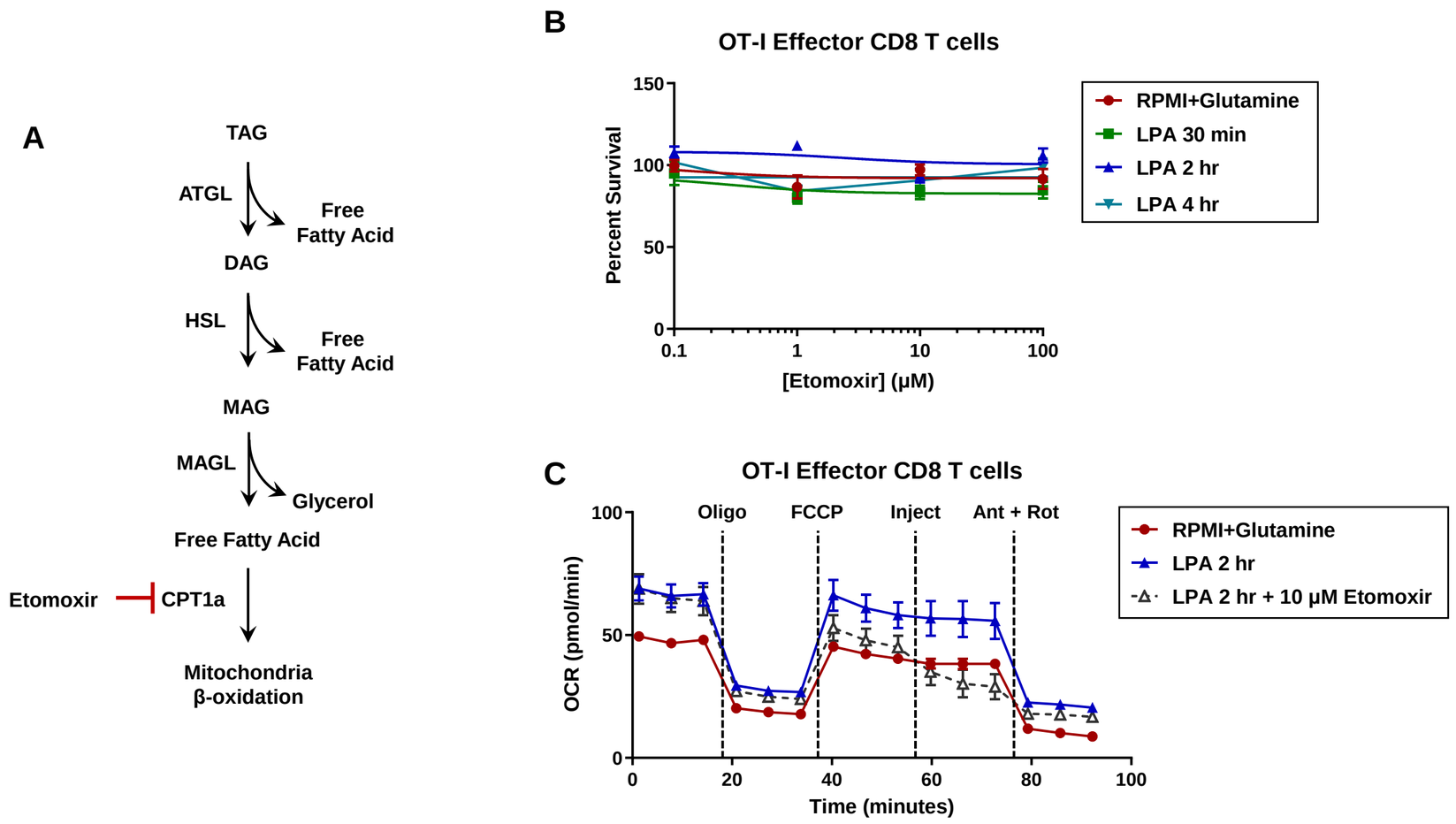

Supplemental Figure 6. Carnitine palmitoyltransferase 1a inhibition abrogates LPA-induced metabolism. (A) Schematic of the lipolytic pathway showing the breakdown and oxidation of lipid droplets. Triacylglycerols (TAG) are found in lipid droplets and are cleaved by adipose triglyceride lipase (ATGL). The product, diacylglycerol (DAG) is further cleaved by hormone sensitive lipase (HSL) to generate monoacylglycerol (MAG). MAG is further cleaved by monoacylglycerol lipase (MAGL) to remove the glycerol backbone. Free fatty acids are transported into the mitochondria for oxidation by carnitine palmitoyltransferase 1a (CPT1a). Translocation of free fatty acids into the mitochondria is the rate-determining step of β-oxidation. CPT1a is inhibited by etomoxir. (B) Day 7 Effector CD8 T cell viability in response to etomoxir. (C) Oxygen consumption rate of day 7 OT-I Effector CD8 T cells treated with either RPMI+Glutmaine or LPA for 2 hours prior to starting the assay. The assay was modified to inject either Seahorse media or etomoxir to a final concentration of 10 μM.

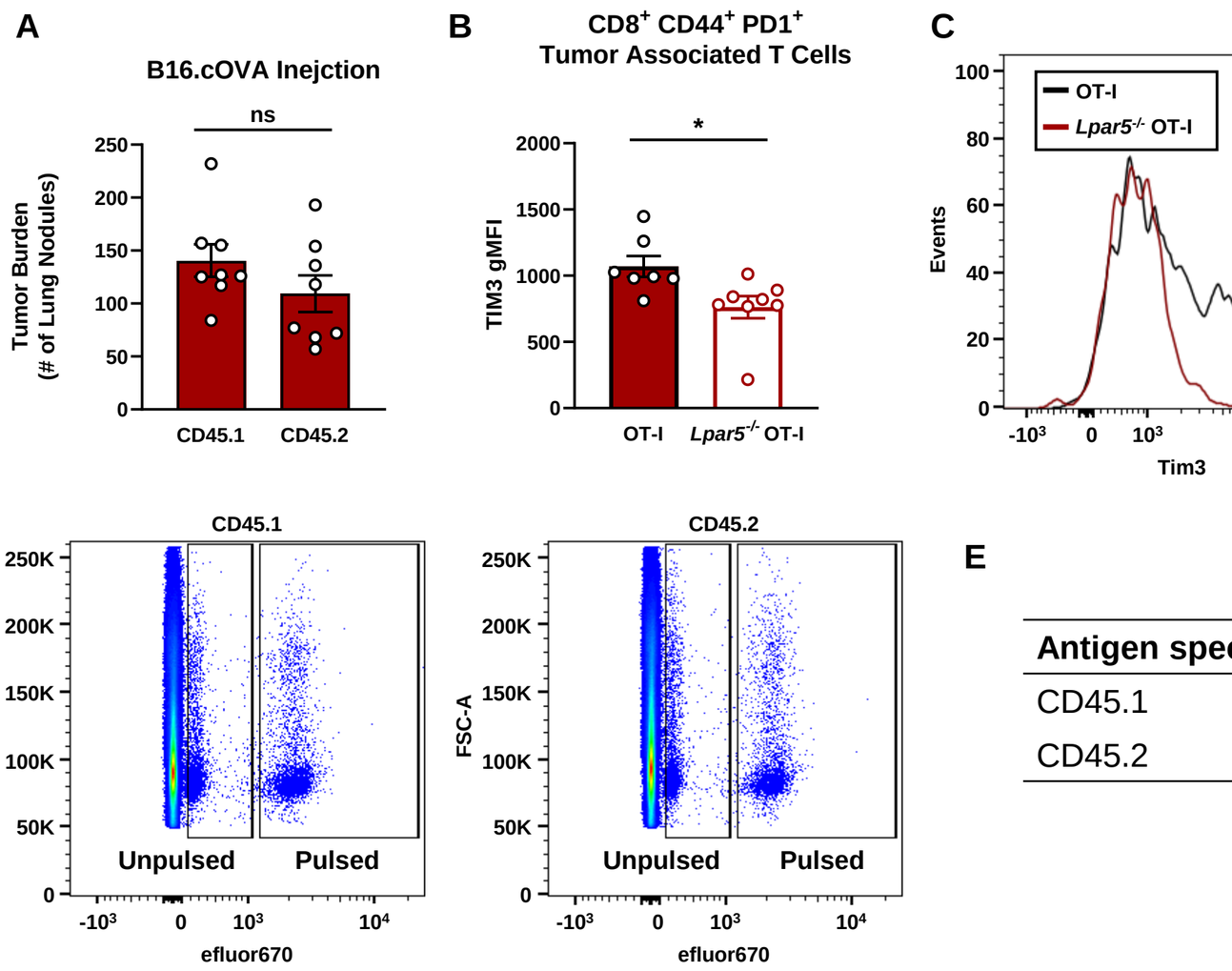

Supplemental Figure 7. LPA phenotype persists in both CD45.1 and CD45.2 backgrounds. (A) Quantitated tumor burden shows no statical difference between mice that received CD45.1 versus CD45.2 OT-I CD8 T cells. (B,C) A reciprocal experiment of congenic markers in adoptive transfer shows that Tim3 expression remains statistically significant. (D,E) There is similar *in vivo* killing between CD45.1 and CD45.2 OT-I CD8 T cells. (F) CD45.1 and CD45.2 OT-I effector CD8 T cells respond similarly to LPA treatment.